Electronic Supplementary Material (ESI) for Environmental Science: Processes & Impacts.

Supplementary File

Including bioconcentration of pesticide metabolites in plant uptake modeling

Zijian Li[a]*, Peter Fantke[b]

[a] School of Public Health (Shenzhen), Sun Yat-sen University, Shenzhen, Guangdong 518107, China. ORCID: http://orcid.org/0000-0002-9291-5966

[b] Quantitative Sustainability Assessment, Department of Environmental and Resource Engineering, Technical University of Denmark, Produktionstorvet 424, 2800 Kgs. Lyngby, Denmark. ORCID: http://orcid.org/0000-0001-7148-6982

* Email: lizijian3@mail.sysu.edu.cn

Table of Contents

S1. Analytical solutions of the general model

The analytical solutions of the general model are derived in this section.

In the soil compartment:

$$Parent\ compound: C_{P,Soil}(t) = C_{P,Soil}(0)\exp\left(-k_{P,Soil}^{Diss}t\right) \tag{s1}$$

$$Metabolite\ i: C_{M,i,Soil}(t) = \frac{k_{M,i,Soil}^{Trans}}{k_{M,i,Soil}^{Diss} - k_{P,Soil}^{Diss}} C_{P,Soil}(0)\left[\exp\left(-k_{P,Soil}^{Diss}t\right) - \exp\left(-k_{M,i,Soil}^{Diss}t\right)\right] \tag{s2}$$

In the tuber compartment:

$$Parent\ compound: C_{P,Tuber}(t) \tag{s3}$$

$$= \frac{k_{P,Tuber}^{S\to T}}{k_{P,Tuber}^{T\to S} + k_{P,Tuber}^{Met} + k_{Tuber}^{Grow} - k_{P,Soil}^{Diss}} C_{P,Soil}(0)\left\{\exp\left(-k_{P,Soil}^{Diss}t\right)\right.$$

$$\left. - \exp\left[-\left(k_{P,Tuber}^{T\to S} + k_{P,Tuber}^{Met} + k_{Tuber}^{Grow}\right)t\right]\right\}$$

$$Metabolite\ i: C_{M,i,Tuber}(t) \tag{s4a}$$

$$= \frac{\frac{k_{M,i,Soil}^{Trans}k_{M,i,Tuber}^{S\to T}}{\left(k_{M,i,Soil}^{Diss} - k_{P,Soil}^{Diss}\right)} + \frac{k_{M,i,Tuber}^{Trans}k_{P,Tuber}^{S\to T}}{\left(k_{P,Tuber}^{T\to S} + k_{P,Tuber}^{Met} + k_{Tuber}^{Grow} - k_{P,Soil}^{Diss}\right)}}{k_{M,i,Tuber}^{T\to S} + k_{M,i,Tuber}^{Met} + k_{Tuber}^{Grow} - k_{P,Soil}^{Diss}} C_{P,Soil}(0)\exp\left(-k_{P,Soil}^{Diss}t\right)$$

$$- \frac{k_{M,i,Tuber}^{S\to T}k_{M,i,Soil}^{Trans}}{\left(k_{M,i,Soil}^{Diss} - k_{P,Soil}^{Diss}\right)\left(k_{M,i,Tuber}^{T\to S} + k_{M,i,Tuber}^{Met} + k_{Tuber}^{Grow} - k_{M,i,Soil}^{Diss}\right)} C_{P,Soil}(0)\exp\left(-k_{M,i,Soil}^{Diss}t\right)$$

$$- \frac{k_{M,i,Tuber}^{Trans}k_{P,Tuber}^{S\to T}}{\left(k_{P,Tuber}^{T\to S} + k_{P,Tuber}^{Met} + k_{Tuber}^{Grow} - k_{P,Soil}^{Diss}\right)\left(k_{M,i,Tuber}^{T\to S} + k_{M,i,Tuber}^{Met} - k_{P,Tuber}^{T\to S} - k_{P,Tuber}^{Met}\right)} C_{P,Soil}(0)\exp\left[-\left(k_{P,Tuber}^{T\to S}\right.\right.$$

$$\left.\left. + k_{P,Tuber}^{Met} + k_{Tuber}^{Grow}\right)t\right] + A\exp\left[-\left(k_{M,i,Tuber}^{T\to S} + k_{M,i,Tuber}^{Met} + k_{Tuber}^{Grow}\right)t\right]$$

$$Integration\ constant: A \tag{s4b}$$

$$= -\frac{\frac{k_{M,i,Soil}^{Trans}k_{M,i,Tuber}^{S\to T}}{\left(k_{M,i,Soil}^{Diss} - k_{P,Soil}^{Diss}\right)} + \frac{k_{M,i,Tuber}^{Trans}k_{P,Tuber}^{S\to T}}{\left(k_{P,Tuber}^{T\to S} + k_{P,Tuber}^{Met} + k_{Tuber}^{Grow} - k_{P,Soil}^{Diss}\right)}}{k_{M,i,Tuber}^{T\to S} + k_{M,i,Tuber}^{Met} + k_{Tuber}^{Grow} - k_{P,Soil}^{Diss}} C_{P,Soil}(0)$$

$$+ \frac{k_{M,i,Tuber}^{S\to T}k_{M,i,Soil}^{Trans}}{\left(k_{M,i,Soil}^{Diss} - k_{P,Soil}^{Diss}\right)\left(k_{M,i,Tuber}^{T\to S} + k_{M,i,Tuber}^{Met} + k_{Tuber}^{Grow} - k_{M,i,Soil}^{Diss}\right)} C_{P,Soil}(0)$$

$$+ \frac{k_{M,i,Tuber}^{Trans}k_{P,Tuber}^{S\to T}}{\left(k_{P,Tuber}^{T\to S} + k_{P,Tuber}^{Met} + k_{Tuber}^{Grow} - k_{P,Soil}^{Diss}\right)\left(k_{M,i,Tuber}^{T\to S} + k_{M,i,Tuber}^{Met} - k_{P,Tuber}^{T\to S} - k_{P,Tuber}^{Met}\right)} C_{P,Soil}(0)$$

where A is the integration constant.

S2. Model application for glyphosate

In this section, we present the calculation process of the rate constants of glyphosate and its primary toxic metabolite (i.e., AMPA).

In the soil compartment:

For the parent compound (glyphosate), the overall dissipation process comprises biodegradation (microorganism), volatilization, water-induced elimination (e.g., surface runoff, and vertical filtration), the uptake by plants (e.g., grasses, weeds), and photolysis (Li, 2021a; Li and Niu, 2021). For the simulation purpose, we only considered the biodegradation process, and other major elimination processes were included in the variability analysis. Thus, the $k_{P,Soil}^{Diss}$ value of glyphosate was approximated as 0.058 d^{-1} (Fantke et al., 2015; Lewis et al., 2016; Li, 2021a), which was based on the biodegradation process in the soil.

For the primary toxic metabolite of glyphosate (AMPA), the overall dissipation process in the soil comprises processes that are similar to those of glyphosate, which is also discussed in the variability analysis. Thus, the $k_{M,i,Soil}^{Diss}$ value of AMPA was approximated as 0.0057 d^{-1} based on the biodegradation process (European Commission, 2020). The $k_{M,i,Soil}^{Trans}$ value of AMPA was estimated as 0.38 d^{-1}, which is the product of the biodegradation rate constant (i.e., 0.058 d^{-1}) and the molecular weight ratio of AMPA to glyphosate (i.e., 0.66) (Li, 2021a).

In the tuber compartment:

The default value of 0.139 d^{-1} was set to k_{Tuber}^{Grow}, which was based on the logistic growth dynamics of the potato (Fantke et al., 2011a; Trapp et al., 2007). Due to little information on the metabolic rate constants of pesticides in plant tissues (Jacobsen et al., 2015; Xiao et al., 2021a, 2021b), we

used half of the dissipation rate constant tabulated by the USEtox database (Fantke et al., 2017), which was estimated as 0.15 d^{-1} for $k_{P,Tuber}^{Met}$. To evaluate the impact of the metabolic kinetics of the compound on simulation results, we conducted the variability analysis in Section S3. In addition, for the same reason, the metabolic rate constant of AMPA in potatoes is unknown; thus, for the risk assessment (Juraske et al., 2011; Trapp et al., 2007), the $k_{M,i,Tuber}^{Met}$ value of AMPA was set as zero. The value $k_{M,i,Tuber}^{Trans}$ of AMPA can be calculated based on the same method for that in the soil, which is estimated as 0.1 d^{-1}, namely the product of the metabolic rate constant of glyphosate in the potato (i.e., $k_{P,Tuber}^{Met} = 0.15$ d^{-1}) and the molecular weight ratio of AMPA to glyphosate (i.e., 0.66).

For the uptake and elimination routes of the compound in potatoes via diffusion, the spherical-shape-based point-estimate approach (Trapp et al., 2007) was adopted to simulate the uptake and elimination rate constants as follows:

$$k_{Tuber}^{S\to T} = \frac{23\theta_{W,T}T_{Tuber}D_W}{r_S{}^2\rho_{Tuber}K_{SW}} \quad \text{(s5)}$$

$$k_{Tuber}^{T\to S} = \frac{23\theta_{W,T}T_{Tuber}D_W}{r_S{}^2\rho_{Tuber}K_{TW}} \quad \text{(s6)}$$

where D_W (m^2 d^{-1}) is the diffusivity of the chemical in water, and the values for glyphosate and AMPA were calculated as 7.5 × 10^{-5} m^2 d^{-1} and 9.3 × 10^{-5} m^2 d^{-1}, respectively, based on the molecular weight approach (Trapp et al., 2003). $\theta_{W,T}$ (dimensionless) is the water content of the tuber tissue, which was estimated as 0.778 (Caetano et al., 2018). T_{Tuber} (dimensionless) is the tortuosity of the tuber tissue, which was estimated as 0.72 (Li, 2021b) based on the water content and air pores of the tuber tissue (Trapp, 2007; Trapp et al., 2007). r_S (m) is the radius of the tuber, which was estimated as 0.04 m based on the medium-sized potato (Trapp et al., 2007). ρ_{Tuber} (kg

L^{-1}) is the density of the tuber (medulla), which was estimated as 1.1 (Li, 2020). K_{SW} (L kg^{-1}) is the soil-water partition coefficient of the compound, which can be estimated according to the major (air, water, and organic matter) components of the soil (Paraíba and Kataguiri, 2008; Trapp et al., 2007) as follows:

$$K_{SW} = \frac{\rho_{S,Dry} f_{OC} K_{OC} + f_W + K_{AW} f_A}{\rho_{S,Wet}} \approx \frac{\rho_{S,Dry} f_{OC} K_{OC} + f_W}{\rho_{S,Wet}} \quad \text{(s7)}$$

where $\rho_{S,Dry}$ (kg L^{-1}) and $\rho_{S,Wet}$ (kg L^{-1}) are the densities of dry and wet soil, respectively, which were estimated as 1.6 kg L^{-1} and 1.95 kg L^{-1}, respectively (Trapp et al., 2007). f_{OC} (dimensionless) is the fraction of the organic matter of the soil, which was estimated as 0.018 (Trapp et al., 2007). f_W (dimensionless) is the water fraction of the soil, which was estimated as 0.28 (Trapp et al., 2007). f_A (dimensionless) is the air fraction of the soil, which was estimated as 0.12 (Trapp et al., 2007). K_{OC} (L kg^{-1}) is the soil sorption partition coefficient of the compound, and the logarithm values ($\log K_{OC}$) of glyphosate and AMPA were taken as 4.34 and 3.7, respectively (Daouk, 2013). K_{AW} (dimensionless) is the air-water partition coefficient (or the dimensionless Henry's law constant) of the compound. We note that the K_{AW} values of glyphosate and AMPA are so low (i.e., non-volatile compounds) that the term '$K_{AW} f_A$' in Eq. (s7) can be negligible (Bento, 2018). Then, the K_{SW} values of glyphosate and AMPA were calculated based on the inputs above as 323 L kg^{-1} and 74.2 L kg^{-1}, respectively. K_{TW} (L kg^{-1}) is the tuber tissue-water partition coefficient of the compound, which can be estimated using the major nutritional components of the tuber (Chiou et al., 2001; Trapp et al., 2007) as follows

$$K_{TW} = 1.22 f_{Lip,T} {K_{OW}}^{0.77} + f_{Carb,T} K_{Ch} + \theta_{W,T} \quad \text{(s8)}$$

where K_{OW} (dimensionless) is the octanol-water partition coefficient of the compound, and the

logarithm values of glyphosate and AMPA were estimated as –3.4 and –1.4, respectively, (National Library of Medicine, 2021; Royal Society of Chemistry, 2022). $f_{Lip,T}$ (dimensionless) and $f_{Carb,T}$ (dimensionless), are the massive contents of lipid and non-lipid carbohydrate, respectively, which were estimated as 0.001 and 0.154, respectively (Trapp et al., 2007). K_{Ch} (L kg^{-1}) is the carbohydrate-water partition coefficient of the compound, and the values of glyphosate and AMPA were estimated (via lipophilicity) as 0.1 (Chiou et al., 2001; Trapp et al., 2007). $\theta_{W,T}$ (L kg^{-1}) is the volumetric content of water in the tuber, which was estimated as 0.778 (Trapp et al., 2007). Then, the K_{TW} values of glyphosate and AMPA were calculated as 0.79.

S3. Variability analysis

The variability analysis was conducted by varying selected rate constants or essential physicochemical properties of glyphosate and AMPA, which generated the variability intervals of the simulation results (e.g., concentrations of the glyphosate and AMPA in the potato). The variability analysis can help users conduct the regional-specific assessment of bioconcentration of pesticides and their toxic metabolites by focusing on site-specific model inputs.

S3.1 Dissipation rate constants of compounds in the soil

In the previous section (i.e., simulating concentrations of glyphosate and AMPA), we only considered the degradation kinetics of glyphosate and AMPA in the soil to estimate the degradation rate constants (i.e., $k_{P,Soil}^{Diss}$ and $k_{M,i,Soil}^{Diss}$) for the conservative consideration (i.e., for the human health risk assessment). However, the overall dissipation of glyphosate and AMPA involves multiple processes. Thus, we varied $k_{P,Soil}^{Diss}$ and $k_{M,i,Soil}^{Diss}$ values of glyphosate and AMPA to generate the variability intervals of the simulated concentrations in the potato. The ranges of $k_{P,Soil}^{Diss}$

and $k_{M,i,Soil}^{Diss}$ values of glyphosate and AMPA were taken as [3.5 × 10^{-3}, 0.7] d^{-1} and [7.2 × 10^{-4}, 3.0 × 10^{-2}] d^{-1}, respectively (Bento, 2018). Accordingly, the $k_{M,i,Soil}^{Trans}$ value of AMPA was estimated by multiplying the half of $k_{P,Soil}^{Diss}$ and 0.66 (i.e., the molecular weight ratio between AMPA and glyphosate). The variability intervals of the simulation results were generated by using the

S3.2 K_{OC} of compounds in the soil

We also varied the K_{OC} values of glyphosate and AMPA to generate the variability intervals of the simulated concentrations of glyphosate and AMPA in the potato because the K_{OC} values can be substantially affected by soil properties (e.g., pH and charges). The ranges of K_{OC} values of glyphosate and AMPA were taken as [884, 60000] L kg^{-1} and [1160, 24800] L kg^{-1}, respectively (Bento, 2018).

S3.3 Metabolic rate constants of compounds in the potato

In the previous section, we set the metabolic rate constant of AMPA as zero for the conservative consideration (i.e., the purpose of the human health risk assessment). However, AMPA can be further biotransformed by plant enzymes (la Cecilia et al., 2018). Thus, we varied the $k_{M,i,Tuber}^{Met}$ value of AMPA in the potato to generate the variability interval of the simulation results. Due to data limitations, we set $k_{M,i,Tuber}^{Met}$ values as 0 d^{-1}, 0.1 d^{-1}, 0.25 d^{-1}, and 0.5 d^{-1}.

S4. Case study

Maggi et al. (2020) evaluated the concentrations of glyphosate and AMPA in global surface soil. We utilized the data of Maggi et al. (2020) (soil residue concentrations) to model the toxic pressure of glyphosate and AMAP in potatoes. The results of the simulation are presented in Table S1. Importantly, certain observed AMPA concentrations in the soil are notably higher than those of

glyphosate, while in other cases, this difference is not evident. This phenomenon arises from the fact that pesticides are usually applied in pulses, and if measurements occur shortly after pesticide application, the parent compounds might exhibit considerably greater soil concentrations than their corresponding metabolites. Additionally, various dynamic environmental factors, including precipitation, wind, sunlight, and humidity, can exert influence on the soil concentrations of chemical contaminants.

Table S1. Summary of glyphosate and AMPA concentration simulation results in potatoes based on their concentrations in global surface soil. The soil concentrations were obtained from Maggi et al. (2020), which were compiled from the scientific literature. Metabolite and non-metabolite models were utilized to calculate glyphosate and AMPA concentrations in potatoes using simulated bioconcentration factors with a 30-day time-to-harvest interval.

Location	Observed (means)		Metabolite model		Non-metabolite model	
	Glyphosate concentration in soil (mg/kg)	AMPA concentration in soil (mg/kg)	Glyphosate concentration in potato (mg/kg)	AMPA concentration in potato (mg/kg)	Glyphosate concentration in potato (mg/kg)	AMPA concentration in potato (mg/kg)
Province of Buenos Aires, Argentina	0.0347	0.2993	2.31E-06	40.99	2.76E-06	34.31
Province of Buenos Aires, Argentina	0.53	0	3.53E-05	0	4.22E-05	0
Toholamni, Western Finland	0.1476	0.1284	9.84E-06	17.58	1.17E-05	14.72
Nntuna, Sweden	0.00965	0.0535	6.43E-07	7.33	7.68E-07	6.13
Lanna, Sweden	0.02147	0.1177	1.43E-06	16.12	1.71E-06	13.49
Sandved, Denmark	0.00081	0.01046	5.40E-08	1.43	6.44E-08	1.20
Montepaldi-San Csciano, Italy	0	0.0609	0	8.34	0	6.98
United Kindom	0.15	0.15	1.00E-05	20.54	1.19E-05	17.20
Denmark	0.11	0.14	7.33E-06	19.17	8.75E-06	16.05
Portugal	1.14	0.73	7.60E-05	99.97	9.07E-05	83.69
Italy	0.13	0.1	8.66E-06	13.70	1.03E-05	11.46
Greece	0.54	0.21	3.60E-05	28.76	4.30E-05	24.08

Spain	0.22	0.09	1.47E-05	12.33	1.75E-05	10.32
Hungary	0.1	0.23	6.67E-06	31.50	7.96E-06	26.37
Poland	0.16	0.14	1.07E-05	19.17	1.27E-05	16.05
Netherland	0.13	0.13	8.66E-06	17.80	1.03E-05	14.90
France	0.08	0.13	5.33E-06	17.80	6.36E-06	14.90
Germany	0.13	0.15	8.66E-06	20.54	1.03E-05	17.20

140

141 **S5. Supplementary figures**

142 The supplementary figures of the main text are provided in this section.

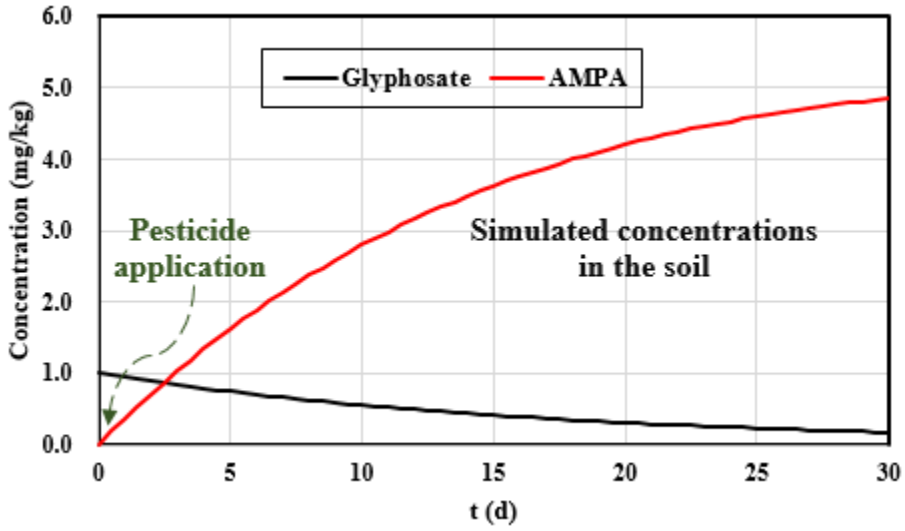

143

144 Figure S1. Simulated concentrations of glyphosate and aminomethylphosphonic acid (AMPA) in

145 the soil based on the initial concentration of glyphosate of 1 mg kg^{-1} in the soil plotted against time

146 (t, d) after pesticide application (i.e., t = 0 d).

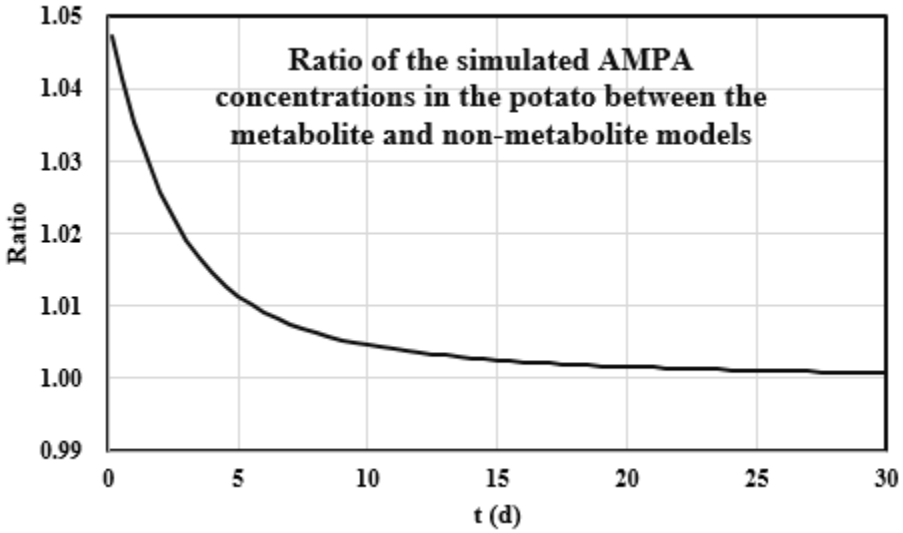

Figure S2. The ratio of the simulated AMPA concentrations in the potato between the metabolite and non-metabolite models plotted against time (t, d) after glyphosate application.

S6. Model extension

In this study, we present a modeling approach that considers the bioconcentration of pesticide metabolites in plants. We demonstrate the effectiveness of this approach using potatoes as an example crop. While there is currently a shortage of experimental studies to evaluate the simulations of pesticides including their metabolites, the plant uptake models, which underlie our proposed approach, have been robustly supported by field observations (Pang et al., 2020, 2016). This robustness lends credibility to our approach for predicting the uptake of organic compounds, encompassing both parent compounds and their metabolites. The modeling experiments utilizing glyphosate as an example serve as a reminder to risk and impact assessors to prioritize the consideration of pesticides' toxic metabolites in addition to the parent compounds. This will contribute to a more comprehensive assessment framework. We note that different plant species have varying pesticide uptake routes that depend on both plant physiology and pesticide

application patterns. However, our proposed modeling approach can be adapted to other crops and their respective pesticide uptake routes. Table S2 provides a summary of the extension of our modeling approach to other crops. Above-ground crops have more pathways for pesticide uptake compared to tuber crops, including surface penetration (such as fruit, leaves, and stems) and transpiration. This is because pesticide residues can be distributed in soil, air, and plant surfaces after their application, particularly through aerial spraying. As a result, pesticide metabolites can be generated in various compartments, which increases their uptake routes by above-ground crops. To simulate metabolite concentrations in above-ground crops, additional equations for metabolite generation compartments and pesticide and metabolite uptake routes are necessary. These equations can be generated and solved using a first-order kinetics-based matrix approach (Fantke et al., 2011b, 2011a). This matrix-based approach offers the capability to provide a comprehensive pesticide bioconcentration or bioaccumulation modeling framework for various plant compartments (including stem, leaf, fruit, and root) across diverse plant species. This allows users to tailor their simulations to edible portions of the plant. For instance, risk assessors may be concerned with pesticide bioconcentration modeling in the leaves of lettuces, while the focus might shift to the fruit of apple trees. With the integration of metabolite simulations into this matrix approach, the added toxicity of metabolites to their parent compounds across all modeling compartments—leaf, fruit, stem, and root—can be generated, which equips users to choose simulation outcomes tailored to any consumable plant parts.

Notably, the PHI for glyphosate application in crops can vary widely, such as ranging from 7 to 28 d (EFSA, 2013). While our simulation results have revealed that the concentration of glyphosate

in potatoes starts to decline shortly after pesticide application (around 2-3 d) and continues to decrease during the potato's growth period, its main metabolite, AMPA, displays a consistent increase in concentration within the potato over a longer period. Therefore, even though certain suggested PHIs for glyphosate might result in reduced pesticide concentrations (e.g., glyphosate itself) at harvest time, their metabolites are likely to accumulate in the edible parts of crops, introducing potentially significant health risks to consumers. Consequently, extending the PHI can indeed help diminish pesticide residue levels in crops. However, this approach warrants careful consideration, particularly for toxic compounds and their metabolites, which could pose substantial health concerns. Hence, it is advisable that the proposed PHI of pesticides, in conjunction with their efficacy in pest management, takes into account the potential adverse effects posed by their metabolites on human and ecological health.

Plant growth dynamics can exert a significant influence on the bioconcentration of pesticides in plant tissues. In this study, we employed a simple yet effective strategy, utilizing the growth rate constant to capture the dilution effect on chemical fate and transport within plants. This approach, widely adopted in modeling and risk assessment endeavors, allows for a straightforward depiction of pesticide behavior (Fantke et al., 2011a; Juraske et al., 2011; Trapp et al., 2007).

The growth and cultivation of crops invariably display region-specific patterns, contributing to the variability of pesticide bioconcentration in plant tissues. As evidenced by our variability analysis, various environmental factors, including soil properties and weather conditions, yield a significant influence on pesticide and metabolite bioconcentration potentials within plants. This is largely attributed to the temperature's substantial impact on the biotransformation rate of the parent

compound. Consequently, an increase in surrounding temperature can lead to a heightened production rate of metabolites. Moreover, given that soil serves as a primary source of pesticide bioconcentration in plants (Fantke et al., 2011a), its composition can significantly differ across regions. For instance, varying soil types possess distinct organic matter contents that directly influence pesticide absorption in the soil. Soils rich in organic matter yield elevated K_{OC} values for lipophilic pesticides, hindering the diffusion kinetics of these compounds from the soil into the tuber. Conversely, diverse pH values in the soil can impact the dissociation process of certain pesticides, particularly those that are ionic or polar in nature (Trapp, 2004). Thus, the uptake of such compounds by plants from the soil will manifest region-specific patterns. To conduct a regional assessment of pesticide and metabolite bioconcentration in plants, we recommend that users modify region-specific model input variables, such as K_{OC}, to generate simulation outcomes that accurately reflect dynamic environmental conditions across regions.

The comparison between metabolite and non-metabolite models reveals that, under specific conditions, such as when plant tissues contain low concentrations of the parent compound or when the biotransformation rate of the parent compound within the plant tissue is notably small, the non-metabolite model can serve as a viable proxy approach. This enables the simulation of the total toxicity equivalent of both the parent compound and its metabolites, especially when the uptake of metabolites from environmental compartments (like soil, air, and plant surfaces) is considered. Given its simplicity and ease of operation, the non-metabolite model is recommended if the aforementioned conditions are met. To ensure this, we suggest performing a preliminary assessment of the degradation kinetics of the parent compound within the plant tissue (Li and

Fantke, 2023). Should the degradation rate constant prove to be relatively low when compared to other uptake or elimination rate constants, opting for the non-metabolite model is advisable, which can facilitate uncomplicated modeling experiments.

Table S2. Summary of notable plant uptake models with their respective metabolite-based modeling strategies.

Crop examples	Plant uptake models	Potential sources of pesticides	Potential sources of pesticide metabolites	References
Lettuce	Grass uptake model	Leaf surface; soil	Leaf surface; soil; plant tissues	(Itoiz et al., 2012; Trapp and Matthies, 1995)
Tomato	Herbaceous uptake model	Leaf surface; soil; fruit surface	Leaf surface; soil; fruit surface; plant tissues	(Juraske et al., 2012, 2007)
Apple	Fruit tree uptake model	Leaf surface; soil; fruit surface; stem surface	Leaf surface; soil; fruit surface; stem surface; plant tissues	(Fantke et al., 2013; Mendez et al., 2018; Trapp, 2007; Trapp et al., 2003)
Carrot	Root crop uptake model	Leaf surface; soil	Leaf surface; soil; plant tissues	(Band and King, 2012; Li, 2022; Trapp, 2002, 2000)

References

Band, L.R., King, J.R., 2012. Multiscale modelling of auxin transport in the plant-root elongation zone. J Math Biol 65. https://doi.org/10.1007/s00285-011-0472-y

Bento, C., 2018. Glyphosate and aminomethylphosphonic acid (AMPA) behavior in loess soils and off-site transport risk assessment. Wageningen University.

Caetano, P.K., Mariano-Nasser, F.A. de C., de MENDONÇA, V.Z., Furlaneto, K.A., Daiuto, E.R., Vieites, R.L., 2018. Physicochemical and sensory characteristics of sweet potato chips undergoing different cooking methods. Food Science and Technology 38. https://doi.org/10.1590/1678-457x.08217

Chiou, C.T., Sheng, G., Manes, M., 2001. A partition-limited model for the plant uptake of organic contaminants from soil and water. Environ Sci Technol. https://doi.org/10.1021/es0017561

Daouk, S., 2013. Fate of the herbicide glyphosate and its metabolite AMPA in soils and their transfer to surface waters : A multi-scale approach in the Lavaux vineyards, western Switzerland. University of Lausanne Open Archive.

European Commission, 2020. EU - Pesticides database [WWW Document]. URL https://ec.europa.eu/food/plant/pesticides/eu-pesticides-database/public/?event=homepage&language=EN (accessed 10.10.20).

Fantke, P., Charles, R., Alencastro, L.F. de, Friedrich, R., Jolliet, O., 2011a. Plant uptake of pesticides and human health: Dynamic modeling of residues in wheat and ingestion intake. Chemosphere. https://doi.org/10.1016/j.chemosphere.2011.08.030

Fantke, P. (Ed.), Bijster, M., Guignard, C., Hauschild, M., Huijbregts, M., Jolliet, O., Kounina, A., Magaud, V., Margni, M., McKone, T.E., Posthuma, L., Rosenbaum, R.K., van de Meent, D., van Zelm, R., 2017. USEtox® 2.0 Documentation (Version 1).

Fantke, P., Huijbregts, M., Margni, M., Hauschild, M., Jolliet, O., McKone, T., Resenbaum, R., Meent, D. van de, 2015. USEtox 2.0 User Manual (v2), USEtox.org.

Fantke, P., Juraske, R., Antón, A., Friedrich, R., Jolliet, O., 2011b. Dynamic multicrop model to characterize impacts of pesticides in food. Environ Sci Technol. https://doi.org/10.1021/es201989d

Fantke, P., Wieland, P., Wannaz, C., Friedrich, R., Jolliet, O., 2013. Dynamics of pesticide uptake into plants: From system functioning to parsimonious modeling. Environmental Modelling and Software. https://doi.org/10.1016/j.envsoft.2012.09.016

Itoiz, E.S., Fantke, P., Juraske, R., Kounina, A., Vallejo, A.A., 2012. Deposition and residues of azoxystrobin and imidacloprid on greenhouse lettuce with implications for human consumption. Chemosphere 89. https://doi.org/10.1016/j.chemosphere.2012.05.066

Jacobsen, R.E., Fantke, P., Trapp, S., 2015. Analysing half-lives for pesticide dissipation in plants. SAR QSAR Environ Res. https://doi.org/10.1080/1062936X.2015.1034772

Juraske, R., Antón, A., Castells, F., Huijbregts, M.A.J., 2007. Human intake fractions of pesticides via greenhouse tomato consumption: Comparing model estimates with measurements for Captan. Chemosphere. https://doi.org/10.1016/j.chemosphere.2006.11.047

Juraske, R., Fantke, P., Ramírez, A.C.R., González, A., 2012. Pesticide residue dynamics in passion fruits: Comparing field trial and modelling results. Chemosphere. https://doi.org/10.1016/j.chemosphere.2012.05.007

Juraske, R., Mosquera Vivas, C.S., Erazo Velásquez, A., García Santos, G., Berdugo Moreno, M.B., Diaz Gomez, J., Binder, C.R., Hellweg, S., Guerrero Dallos, J.A., 2011. Pesticide uptake in potatoes: Model and field experiments. Environ Sci Technol. https://doi.org/10.1021/es102907v

la Cecilia, D., Tang, F.H.M., Coleman, N. v., Conoley, C., Vervoort, R.W., Maggi, F., 2018. Glyphosate dispersion, degradation, and aquifer contamination in vineyards and wheat fields in the Po Valley, Italy. Water Res 146. https://doi.org/10.1016/j.watres.2018.09.008

Lewis, K.A., Tzilivakis, J., Warner, D.J., Green, A., 2016. An international database for pesticide risk assessments and management. Human and Ecological Risk Assessment. https://doi.org/10.1080/10807039.2015.1133242

Li, Z., 2022. Modeling plant uptake of organic contaminants by root vegetables: The role of diffusion, xylem, and phloem uptake routes. J Hazard Mater 434, 128911. https://doi.org/10.1016/j.jhazmat.2022.128911

Li, Z., 2021a. Improving screening model of pesticide risk assessment in surface soils: Considering degradation metabolites. Ecotoxicol Environ Saf 222. https://doi.org/10.1016/j.ecoenv.2021.112490

Li, Z., 2021b. Regulation of pesticide soil standards for protecting human health based on multiple uses of residential soil. J Environ Manage 297. https://doi.org/10.1016/j.jenvman.2021.113369

Li, Z., 2020. A coupled ODE-diffusion modeling framework for removing organic contaminants in crops using a simple household method. Environmental Pollution 265, 115071. https://doi.org/10.1016/j.envpol.2020.115071

Li, Z., Fantke, P., 2023. Considering degradation kinetics of pesticides in plant uptake models: proof of concept for potato. Pest Manag Sci 79, 1154–1163. https://doi.org/10.1002/ps.7288

Li, Z., Niu, S., 2021. Modeling pesticides in global surface soils: Evaluating spatiotemporal patterns for USEtox-based steady-state concentrations. Science of The Total Environment 791. https://doi.org/10.1016/j.scitotenv.2021.148412

Maggi, F., la Cecilia, D., Tang, F.H.M., McBratney, A., 2020. The global environmental hazard of glyphosate use. Science of The Total Environment 717, 137167. https://doi.org/10.1016/j.scitotenv.2020.137167

Mendez, A., Castillo, L.E., Ruepert, C., Hungerbuehler, K., Ng, C.A., 2018. Tracking pesticide fate in conventional banana cultivation in Costa Rica: A disconnect between protecting ecosystems and consumer health. Science of the Total Environment 613–614. https://doi.org/10.1016/j.scitotenv.2017.09.172

National Library of Medicine, 2021. PubChem [WWW Document]. URL https://pubchem.ncbi.nlm.nih.gov/ (accessed 5.1.21).

Pang, N., Cui, Y., Hu, J., 2016. Weather dependent dynamics of the herbicides florasulam, carfentrazone-ethyl, fluroxypyr-meptyl and fluroxypyr in wheat fields through field studies and computational simulation. Chemosphere 165. https://doi.org/10.1016/j.chemosphere.2016.09.026

Pang, N., Fan, X., Fantke, P., Zhao, S., Hu, J., 2020. Dynamics and dietary risk assessment of thiamethoxam in wheat, lettuce and tomato using field experiments and computational simulation. Environmental Pollution 256. https://doi.org/10.1016/j.envpol.2019.113285

Paraíba, L.C., Kataguiri, K., 2008. Model approach for estimating potato pesticide bioconcentration factor. Chemosphere. https://doi.org/10.1016/j.chemosphere.2008.07.026

Reasoned opinion on the import tolerance for glyphosate in genetically modified oilseed rape, 2013. . EFSA Journal 11. https://doi.org/10.2903/j.efsa.2013.3456

Royal Society of Chemistry, 2022. Search ChemSpider [WWW Document].
Trapp, S., 2007. Fruit tree model for uptake of organic compounds from soil and air. SAR QSAR Environ Res. https://doi.org/10.1080/10629360701303693
Trapp, S., 2004. Plant Uptake and Transport Models for Neutral and Ionic Chemicals. Environmental Science and Pollution Research. https://doi.org/10.1065/espr2003.08.169
Trapp, S., 2002. Dynamic root uptake model for neutral lipophilic organics. Environ Toxicol Chem 21. https://doi.org/10.1002/etc.5620210128
Trapp, S., 2000. Modelling uptake into roots and subsequent translocation of neutral and ionisable organic compounds. Pest Manag Sci 56, 767–778. https://doi.org/10.1002/1526-4998(200009)56:9<767::AID-PS198>3.0.CO;2-Q
Trapp, S., Cammarano, A., Capri, E., Reichenberg, F., Mayer, P., 2007. Diffusion of PAH in potato and carrot slices and application for a potato model. Environ Sci Technol. https://doi.org/10.1021/es062418o
Trapp, S., Matthies, M., 1995. Generic One-Compartment Model for Uptake of Organic Chemicals by Foliar Vegetation. Environ Sci Technol. https://doi.org/10.1021/es00009a027
Trapp, S., Rasmussen, D., Samsøe-Petersen, L., 2003. Fruit tree model for uptake of organic compounds from soil. SAR QSAR Environ Res. https://doi.org/10.1080/1062936021000058755
Xiao, S., Gong, Y., Li, Z., Fantke, P., 2021a. Improving Pesticide Uptake Modeling into Potatoes: Considering Tuber Growth Dynamics. J Agric Food Chem. https://doi.org/10.1021/acs.jafc.1c00151
Xiao, S., Li, Z., Fantke, P., 2021b. Improved plant bioconcentration modeling of pesticides: The role of periderm dynamics. Pest Manag Sci. https://doi.org/10.1002/ps.6549